

NATIONAL ADVISORY COMMITTEE FOR AERONAUTICS

**WARTIME REPORT**

ORIGINALLY ISSUED  
September 1942 as  
Advance XXXXXXXXXX Report

WIND-TUNNEL INVESTIGATION OF A PLAIN AILERON WITH  
VARIOUS TRAILING-EDGE MODIFICATIONS ON A TAPERED WING

I - AILERON WITH FIXED INSET TABS

By F. M. Rogallo and Paul E. Purser

Langley Memorial Aeronautical Laboratory  
Langley Field, Va.



WASHINGTON

NACA WARTIME REPORTS are reprints of papers originally issued to provide rapid distribution of advance research results to an authorized group requiring them for the war effort. They were previously held under a security status but are now unclassified. Some of these reports were not technically edited. All have been reproduced without change in order to expedite general distribution.

NATIONAL ADVISORY COMMITTEE FOR AERONAUTICS

ADVANCE [REDACTED] REPORT

WIND-TUNNEL INVESTIGATION OF A PLAIN AILERON WITH  
VARIOUS TRAILING-EDGE MODIFICATIONS ON A TAPERED WING

I - AILERON WITH FIXED INSET TABS

By F. M. Rogallo and Paul E. Purser

SUMMARY

An investigation was made in the LMAL 7- by 10-foot tunnel of various modifications to the trailing edge of a 0.255-chord, plain aileron on a semispan model of the tapered wing of a fighter airplane. The modifications considered in the present report were: (1) plain and up-rigged ailerons with fixed positive tabs to provide up-floating tendencies and allow reduction of stick force through the use of conventional differential aileron linkages; and (2) plain and downrigged ailerons with fixed negative tabs to provide downfloating tendencies and allow reductions of stick force through the use of reversed differential aileron linkages. The effect of a gap at the aileron nose was investigated for each of the basic modifications.

Stick forces and rates of roll were estimated for a fighter airplane with the plain and with the modified ailerons. The computed characteristics indicated that for the arrangement tested the use of ailerons with fixed inset tabs combined with a suitable differential aileron linkage will reduce the maximum stick forces to 40 percent or less of those experienced in the use of plain ailerons with an equal up-and-down-aileron linkage. The decrease in stick force was greater and the change in aileron effectiveness was less for the ailerons with positive tabs than for the ailerons with negative tabs. The results indicated that the presence of a gap at the aileron nose and also the use of initial aileron deflection to counteract the lift increment due to tab deflection were detrimental to the aileron effectiveness and to the stick-force characteristics.

L-513

## INTRODUCTION

In view of the increased importance of obtaining adequate lateral control with reasonable stick forces under all flight conditions for high-speed airplanes, the NACA has engaged in an extensive program of lateral-control research. The purposes of this program are to develop new lateral-control devices and to determine more accurately the characteristics of various modifications of existing devices,

L-513

In the present; investigations tests were made of 0.155-chord ailerons with positive and negative fixed inset tabs, which may be considered as simulating ailerons with drooped or reflexed trailing edges and with sealed and unsealed gaps. In the analysis of the data, the cases of uprigged ailerons with positive tabs, downrigged ailerons with negative tabs, and neutrally rigged ailerons with positive and negative tabs were considered. For the uprigged and downrigged ailerons, the aileron angle in the neutral position was such as to compensate approximately for the lift change due to the tab deflection.

## APPARATUS AND METHODS

### Test Installation

A semispan-wing model was suspended in the LMAL 7- by 10-foot tunnel (reference 1) as shown schematically in figure 1. The root chord of the model was adjacent to one of the vertical walls of the tunnel, the vertical wall thereby serving as a reflection plane. The flow over a semispan in this set-up is essentially the same as it would be over a complete wing in a 7- by 20-foot tunnel. Although a very small clearance was maintained between the root chord of the model and the tunnel wall, no part of the model was fastened to or in contact with the tunnel wall. The model was suspended entirely from the balance frame, as shown in figure 1, in such a way that all the forces and moments acting on it might be determined. Provision was made for changing the angle of attack while the tunnel was in operation.

The ailerons were deflected by means of a calibrated torque rod connecting the outboard end of the aileron with a crank outside the tunnel wall and the hinge moments were determined from the twist of the rod (fig. 1).

## Models

The tapered-wing model used in these tests was built to the plan form shown in figure 2 and represents the cross-hatched portion of the airplane shown in figure 3. The basic airfoil sections were of the NACA 230 series tapering in thickness from approximately 15½ percent at the root to 8¼ percent at the tip (table I). The basic chord  $c_1$  of the model was increased 0.3 inch to reduce the trailing-edge thickness and the last few stations were refaired to give a smooth contour. The details of the ailerons and the tabs are shown in figure 4. Figure 5 is a diagrammatic comparison of the actual ailerons and the ailerons that they were intended to simulate.

## Test Conditions

All the tests were made at a dynamic pressure of 9.21 pounds per square foot, which corresponds to a velocity of about 60 miles per hour and to a test Reynolds number of about 1,543,000 based on the wing mean aerodynamic chord of 33.66 inches. The effective Reynolds number of the tests was about 2,460,000 based on a turbulence factor of 1.6 for the LMAL 7- by 10-foot tunnel. The present tests were made at low scale, low velocity, and high turbulence relative to flight conditions to which the results are applied. The effects of these variables were not determined or estimated.

## RESULTS AND DISCUSSION

### Coefficients and Corrections

The symbols used in the presentation of results are:

$C_L$  lift coefficient ( $L/qS$ )

$C_D$  uncorrected drag coefficient ( $D/qS$ )

$C_m$	pitching-moment coefficient ( $M/qSc'$ )
$C_l'$	rolling-moment coefficient ( $L'/qbS$ )
$C_n'$	yawing-moment coefficient ( $N'/qbS$ )
$C_h$	aileron hinge-moment coefficient ( $H/qb_a \bar{c}_a^2$ )
$c$	actual wing chord at any spanwise location
$c_1$	chord of basic airfoil section at any spanwise location
$c'$	mean aerodynamic chord
$c_a$	aileron chord measured along airfoil chord line from hinge axis of aileron to trailing edge of airfoil
$\bar{c}$	root-mean-square chord of the aileron
$b$	twice span of semispan model
$b_a$	aileron span
$S$	twice area of semispan model
$L$	twice lift on semispan model
$D$	twice drag on semispan model
$M$	twice pitching moment of semispan model about support axis
$L'$	rolling moment, due to aileron deflection, about wind axis in plane of symmetry
$N'$	yawing moment, due to aileron deflection, about wind axis in plane of symmetry
$H$	aileron hinge moment
$q$	dynamic pressure of air stream uncorrected for blocking $\left(\frac{1}{2}\rho V^2\right)$
$V$	free-stream velocity
$V_i$	indicated velocity

- $a$  angle of attack
- $\delta_a$  aileron deflection relative to wing, positive when trailing edge is down
- $\delta_{a_i}$  initial aileron deflection (for neutral position) relative to wing, positive when trailing edge is down
- $\delta_t$  tab deflection relative to aileron, positive when trailing edge is down
- $\theta_s$  control-stick deflection
- $C_l'p$  rate of change of rolling-moment coefficient  $C_l'$  with helix angle  $pb/2V$
- $p$  rate of roll
- $F_s$  stick force

A positive value of  $L'$  or  $C_l'$  corresponds to an increase in lift of the model, and a positive value of  $N'$  or  $C_n'$  corresponds to a decrease in drag of the model. Twice the actual lift, drag, pitching moment, area, and span of the model were used in the reduction of the results because the model represented half a complete wing. The drag coefficient and the angle of attack have been corrected only in accordance with the theory of trailing-vortex images. Corresponding corrections were applied to the rolling- and yawing-moment coefficients. No correction has been applied to the hinge-moment coefficients. No corrections have been applied to any of the results for blocking, for the effects of the support strut, or for the treatment of the inboard end of the wing; that is, the small gap between the wing and the wall, the leakage through the wall around the support tube, and the boundary layer at the wall. These effects are probably of second-order importance for the rolling- and yawing-moment coefficients (which are basically incremental data.) but may have more effect on the other forces and moments, particularly on the drag coefficients. It is for this reason that the drag coefficients are referred to as uncorrected.

### Characteristics of Model with Aileron Neutral

The characteristics of the wing model with the plain aileron fixed at zero are shown in figure 6.

Similar data were not obtained directly for the wing model with the various modified ailerons fixed at zero; the characteristics of the model with these ailerons were obtained by replotting the data obtained in tests of the aileron with a full-span fixed tab. For the uprigged and downrigged ailerons with fixed positive and negative tabs the aileron deflections were adjusted to counteract the lift due to tab deflection at an angle of attack of about  $0.1^\circ$ . The adjustments, however, did not exactly counteract the lift due to the tab at high angles of attack or the drag due to the tab at high or low angles of attack. The rolling and yawing moments due to tab and initial aileron deflection would be of opposite sign for the right and left ailerons and would appear on the airplane as increments in lift and drag only.

L-513

### Aileron Characteristics

Plain ailerons.— The characteristics of the plain sealed and unsealed ailerons are presented in figure 7. A comparison of the results shows that at  $\delta_a = \pm 15^\circ$  the presence of a 0.005c gap at the aileron nose reduced the effectiveness of the aileron by about 16 percent and increased the hinge-moment increment by about 12 percent but had little effect on the slope of the hinge-moment curve  $\partial C_h / \partial \delta_a$  at small deflections.

Uprigged ailerons with positive tabs.— The characteristics of the uprigged ailerons with positive tabs are presented for sealed and unsealed gaps in figures 8 and 9, respectively. The ailerons with sealed gaps had larger floating angles than those with unsealed gaps and also had a more regular increase in floating angle with tab deflection. As anticipated from the plain aileron tests, the sealed ailerons were also more effective than the ailerons with the 0.005c gaps.

Downrigged ailerons with negative tabs.— The characteristics of the downrigged ailerons with negative tabs are shown for sealed and unsealed gaps in figures 10 and 11, respectively. The sealed ailerons again were more effective than those with the unsealed gaps and had

larger floating angles and more regular variation of floating angle with tab deflection. The upfloating angles of the uprigged ailerons were larger than the downfloating angles of the downrigged ailerons. The tab stalled at smaller aileron deflections and produced hinge-moment curves that were much more irregular for the downrigged ailerons than for the uprigged ailerons and also caused a loss in effectiveness for the downrigged ailerons.

The ratio of adverse yawing moment to rolling moment at a high angle of attack was larger for the downrigged ailerons than for the plain and uprigged ailerons. The data of reference 2 indicate that the importance of aileron yawing moments is greatly dependent upon the characteristics of the individual airplane and that the ill effects of adverse aileron yawing moment tend to disappear as the weathercock stability of the airplane is increased and as the effective dihedral is decreased.

Neutrally rigged ailerons with tabs.— In order to reduce the loss of effectiveness of the downrigged ailerons and to increase the floating angles of both the uprigged and the downrigged ailerons, the ailerons were assumed to be neutrally rigged and the data of figures 8 and 10 were replotted with no initial aileron deflection; that is, the ailerons were not deflected to counteract the lift increment due to tab deflection. These data are presented for tabs deflected positively and negatively in figures 12 and 13, respectively.

#### Estimated Rates of Roll and Stick Forces

In order to take advantage of the floating tendencies of the ailerons, two differential linkages were designed and their characteristics are presented in figure 14,

The rates of roll and the stick forces during steady rolling of the airplane of figure 3 have been estimated from the data of figures 7 to 13. The rates of roll were estimated by means of the relationship

$$p b / 2 V = C_{l'} / C_{l'} p \quad (1)$$

where the coefficient of damping in roll  $C_{l'} p$  was taken as 0.46 from the data of reference 3. It has been assumed that the rudder will be used to counteract the yawing



moment and wing twist has been neglected. The stick forces were estimated from the relationship

$$F_s = \frac{90.3}{C_L} \left[ C_{h_d} \left( \frac{d\delta_a}{d\theta_s} \right)_d - C_{h_u} \left( \frac{d\delta_a}{d\theta_s} \right)_u \right] \quad (2)$$

which may be derived from the aileron dimensions and the following airplane characteristics:

Wing area, sq ft . . . . .	260
Span, ft . . . . .	38
Taper ratio . . . . .	4.87:1
Airfoil section (basic) . . . . .	NACA 230 series
Mean aerodynamic chord, in. . . . .	84.14
Weight, lb . . . . .	7063
Wing loading, lb/sq ft . . . . .	27.2
Stick length, ft . . . . .	2
Maximum stick deflection, $\theta_s$ , deg . . . . .	$\pm 21$
Maximum total aileron deflection, deg (up aileron plus down aileron) . . . . .	32

The value of the constant in equation (2) is dependent upon the wing loading, the size of the ailerons, and the length of the stick. The subscripts u and d refer to the up and down ailerons, respectively. The values of  $d\delta_a/d\theta_s$  were determined from figure 14 for the differential linkages and had a constant value of  $-16/21$  for the equal up-and-down linkage. The values of  $C_{l'}$  and  $C_h$  used in equations (1) and (2) are the values thought to exist during steady rolling; the difference in angle of attack of the two ailerons due to rolling has been taken into account. In order to be able to take into account the difference in angle of attack of the two ailerons, the rolling- and hinge-moment coefficients were replotted against angle of attack for several aileron deflections, and the fairing between the points at  $\alpha = 0.11^\circ$  and the points at  $\alpha = 13.35^\circ$  was guided by the fairing of the curves for the plain aileron, which were cross plots of figure 7(b).

When an aileron has an upfloating tendency, the use of a properly designed differential linkage will reduce the high-speed stick forces, but, since the upfloating angle of the aileron usually increases as the speed is reduced, the differential becomes more effective and the stick forces may be overbalanced at low speeds. This

5.55-11  
344  
13002  
11522

04  
4

L-513

tendency may be overcome by designing the differential for the largest upfloating angle that the aileron is expected to have (references 4 and 5), but the system will still have a large variation of stick force with speed. It was thought that reversing the differential and giving the aileron a downfloating angle which would decrease instead of increase as the speed was reduced would give the system a smaller variation of stick force with speed. A comparison of figures 15 and 17 or of figures 16 and 18, however, shows that the results of the stick-force computations do not strongly support the preceding analysis. The somewhat disappointing results are ascribed to the facts that the variation of aileron floating angle with angle of attack is small for this model, that the down-rigged ailerons with negative tabs were less effective and had steeper and more irregular hinge-moment curves than the uprigged ailerons with positive tabs, and that the tabs on all arrangements were less effective at high than at low angles of attack.

It is thought, that on low-drag airfoils, where the variation of floating angle with angle of attack is much greater than on the NACA 230 series, the reverse differential and negative tab would have better stick-force characteristics than the conventional differential and positive tab. A comparison of figures 15 and 37 with figure 19 shows that eliminating the initial deflection of the ailerons increased their effectiveness and, because of the larger floating angles, reduced the maximum high-speed stick forces to about 30 or 35 pounds. The neutrally rigged aileron with the  $-20^\circ$  tab, however, was overbalanced for the low-speed condition. This unforeseen circumstance was caused by the fact that, at the high angle of attack, the tab was partly stalled for all negative aileron deflections and for positive deflections up to nearly  $10^\circ$ . (See fig. 13(b).) The estimated hinge-moment-coefficient curve of figure 13(b) was based on the assumption that the tab stall would be delayed considerably by increasing the Reynolds number to that of flight conditions and by using a smoother aileron-tab juncture than that used in the present tests. This last assumption is justified by the unpublished results of tests of ailerons with beveled trailing edges in which rounding the corners of the bevel resulted in an improvement in the aileron characteristics. A comparison between the actual and the simulated ailerons (fig. 5) should be similar to a comparison of the ailerons with sharp and with rounded bevel corners. The stick forces which were computed

using the estimated hinge-moment-coefficient curve of figure 13(b) were not overbalanced at low speed. (See fig. 19.) Although no corresponding rolling-moment coefficients were estimated, it is probable that: such an estimated curve would show a larger aileron effectiveness than do the curves of figures 13(b) and 19.

### CONCLUSIONS

The results of the tests of 0.155-chord ailerons on an NACA 230 series airfoil and the computations indicated that, for the arrangement tested, the use of ailerons with fixed inset tabs combined with a suitable differential aileron linkage can reduce the maximum stick forces to about 40 percent or less of the forces experienced in the use of plain ailerons with an equal up-and-down linkage. The decreases in stick forces were greater and the changes in aileron effectiveness were less for the ailerons with positive tabs than for the ailerons with negative tabs. The results indicated that the presence of a gap at the aileron nose and also the use of initial aileron deflection to counteract the lift increment due to tab deflection were detrimental to the aileron effectiveness and to the stick-force characteristics.

Langley Memorial Aeronautical Laboratory,  
National Advisory Committee for Aeronautics,  
Langley Field, Va.

1-513

## REFERENCES

- ✓ 1. Wenzinger, Carl J., and Harris, Thomas A.: Wind-Tunnel Investigation of an N.A.C.A. 23012 Airfoil with Various Arrangements of Slotted Flaps. Rep. No. 664, NACA, 1939.
- " 2. Fehlnner, Leo F.: A Study of the Effects of Vertical Tail Area and Dihedral on the Lateral Maneuverability of an Airplane. NACA A.R.R., Oct. 1941.
- ✓ 3. Gilruth, R.R., and Turner, W.N.: Lateral Control Required for Satisfactory Flying Qualities Based on Flight Tests of Numerous Airplanes. Rep. No. 715, NACA, 1941,
- ✓ 4. Jones, Robert T., and Nerken, Albert I.: The Reduction of Aileron Operating Force by Differential Linkage. T.N. No. 586, NACA, 1936.
- ✓ 5. Soulé, H. A., and Hootman, James A.: A Flight Investigation of the Reduction of Aileron Operating Force by Means of Fixed Tabs and Differential Linkage, with Notes on Linkage Design. T.N. No. 653, NACA, 1938.

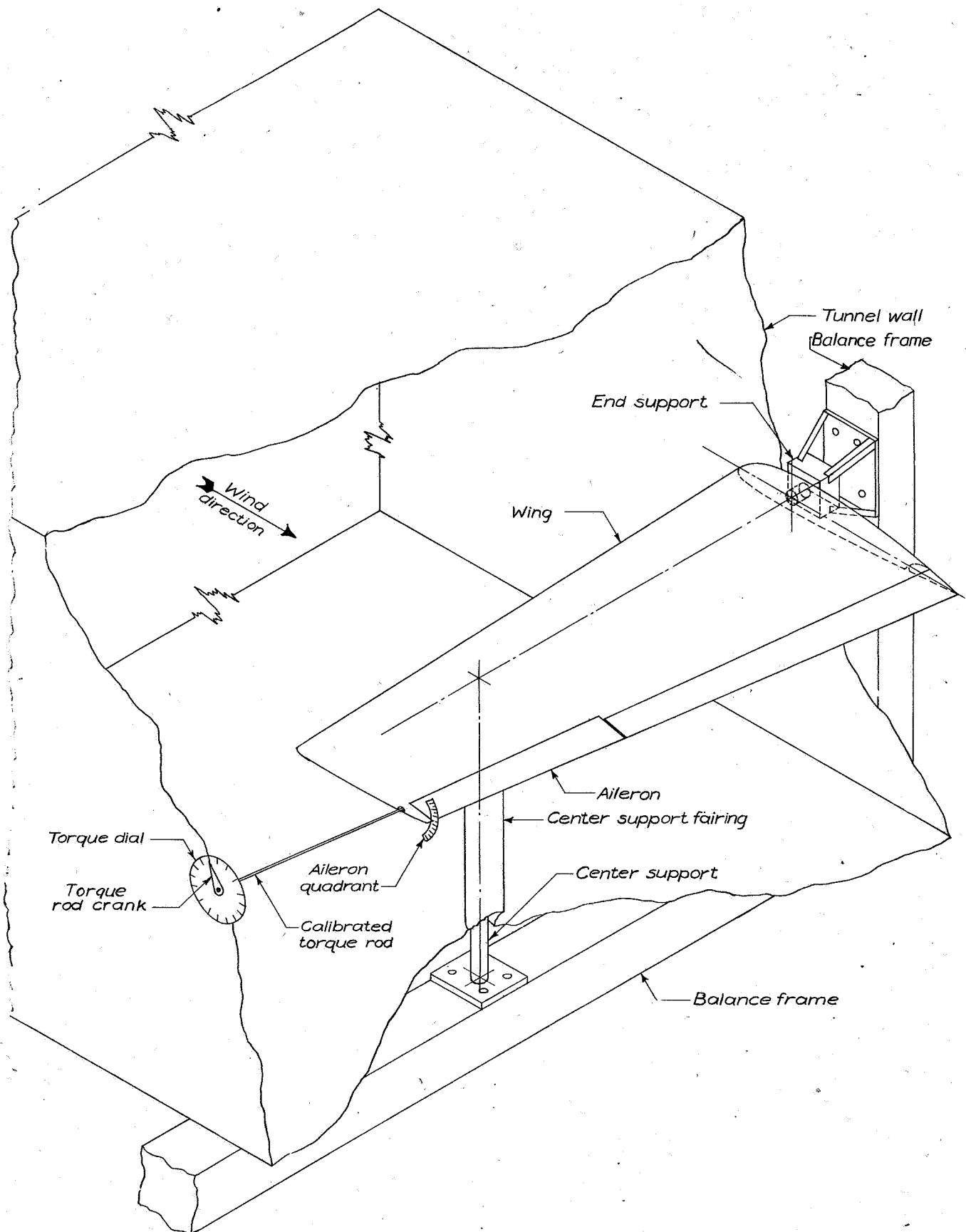


Figure 1.- Schematic diagram of test installation.

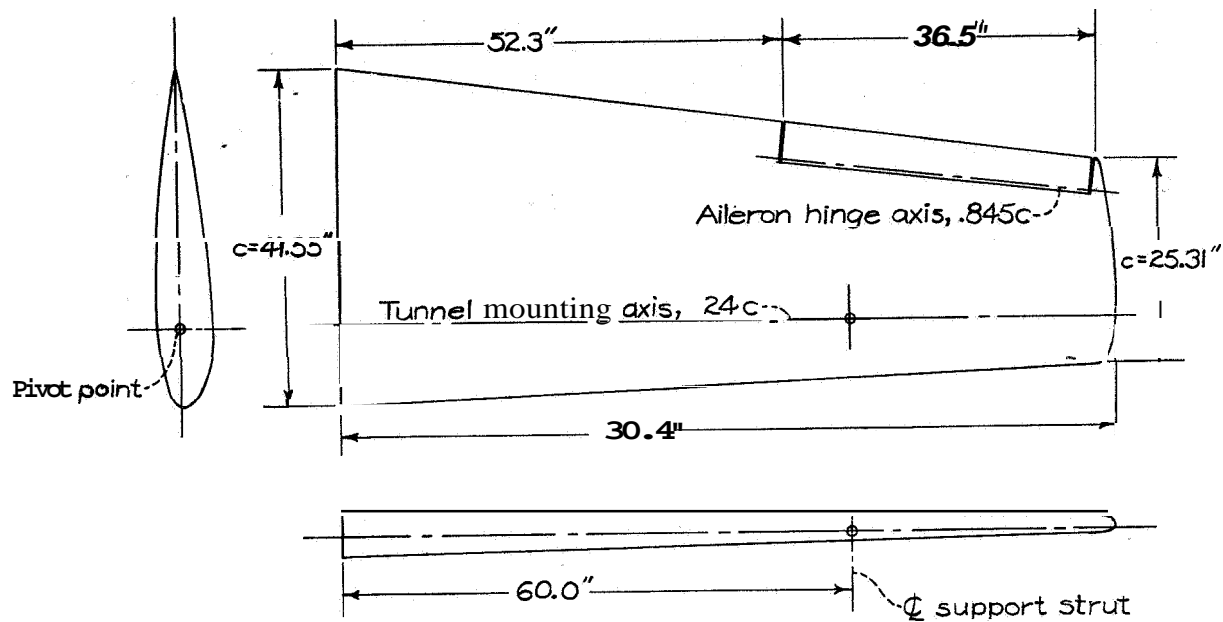


Figure 2.- Semispan model of tapered wing.

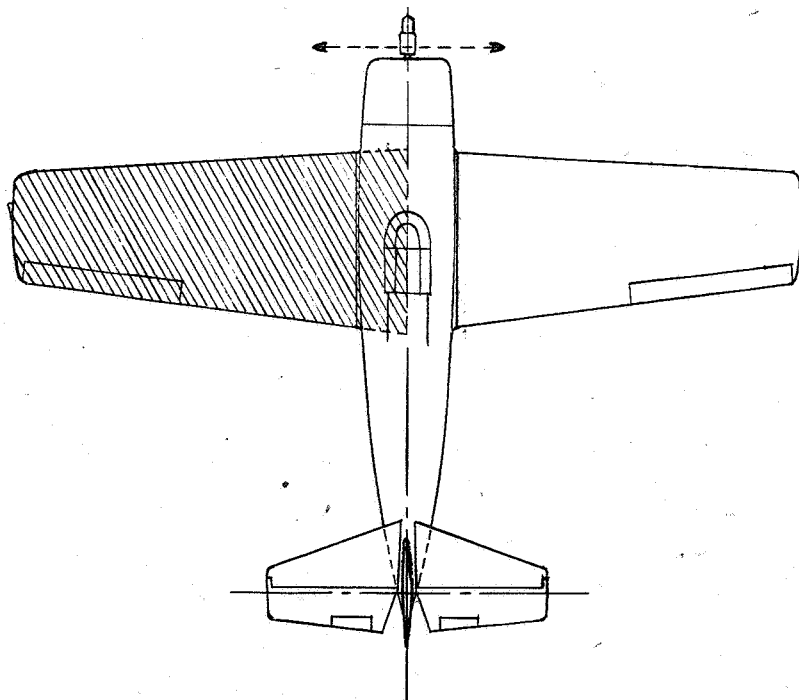


Figure 3.- Portion of airplane simulated by model.

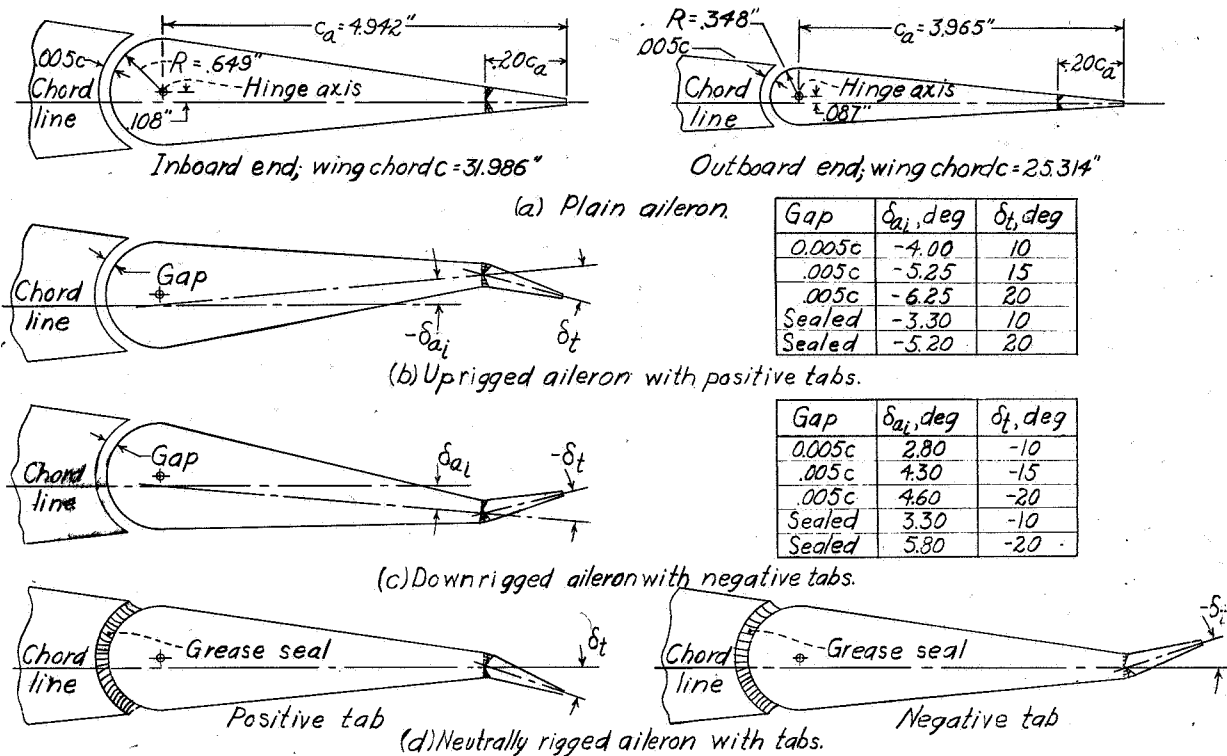


Figure 4.- The various 0.155 c by 0.405 b/2 ailerons with 0.20 c\_a by 1.0 b\_a fixed inset tabs tested on the tapered-wing model.

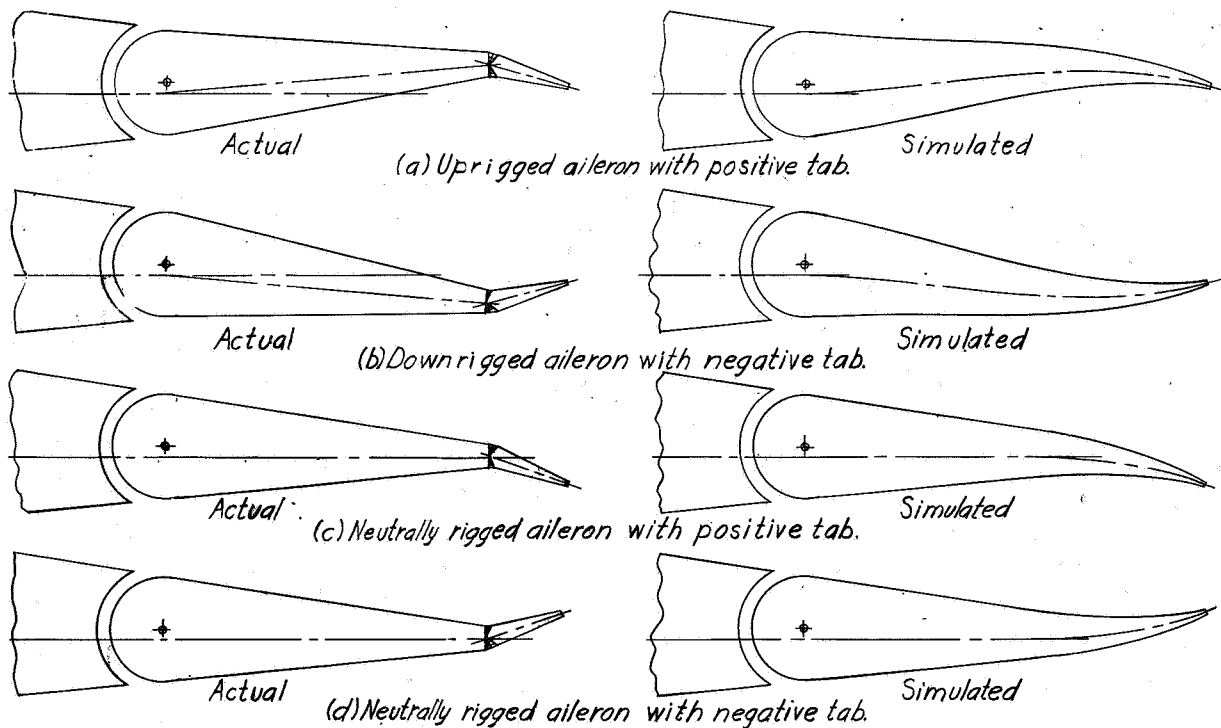


Figure 5.- Comparison of actual and simulated ailerons.

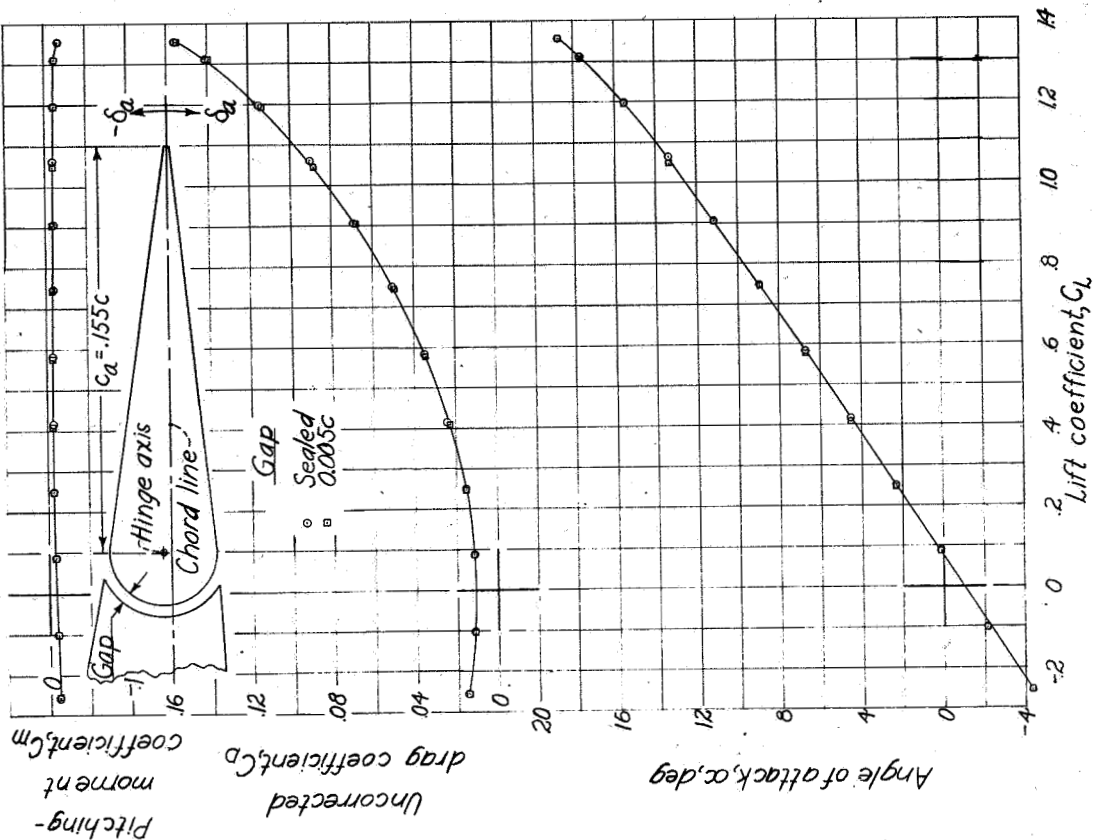
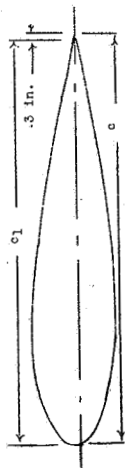


Figure 6.-Characteristics of the tapered-wing model with the plain aileron fixed at zero.

TABLE I  
ORDINATES FOR AIRFOIL

Spanwise stations in inches from root section. Chord stations and ordinates in percent of basic wing chord  $c_1$



Model wing station 0			Model wing station 86.8		
Station	Upper surface	Lower surface	Station	Upper surface	Lower surface
0	3.48	-1.00	0	1.89	-1.34
1.25	4.61	-2.36	1.25	2.68	-1.07
2.5	6.10	-3.21	2.5	3.70	-1.26
5	7.14	-3.82	5	4.93	-1.46
7.5	7.89	-4.32	7.5	5.54	-1.66
10	8.22	-4.71	10	5.77	-1.82
15	8.40	-5.10	15	5.77	-2.02
20	8.37	-5.28	20	5.71	-2.26
25	8.32	-5.78	25	5.38	-2.52
30	8.26	-6.00	30	4.08	-2.57
40	8.12	-6.97	40	3.21	-1.87
50	7.97	-7.67	50	2.26	-1.35
60	7.82	-8.16	60	1.22	-0.78
70	7.67	-8.46	70	0.70	-0.46
80	7.52	-8.71	80	0.15	-0.14
90	7.37	-8.91	90	0.05	-0.05
95	7.22	-9.06			
100	7.07	-9.21			
100.73	6.92	-9.36			

L.E. radius: 0.70. Slope of radius through end of chord: 0.305

L.E. radius: 2.65. Slope of radius through end of chord: 0.305



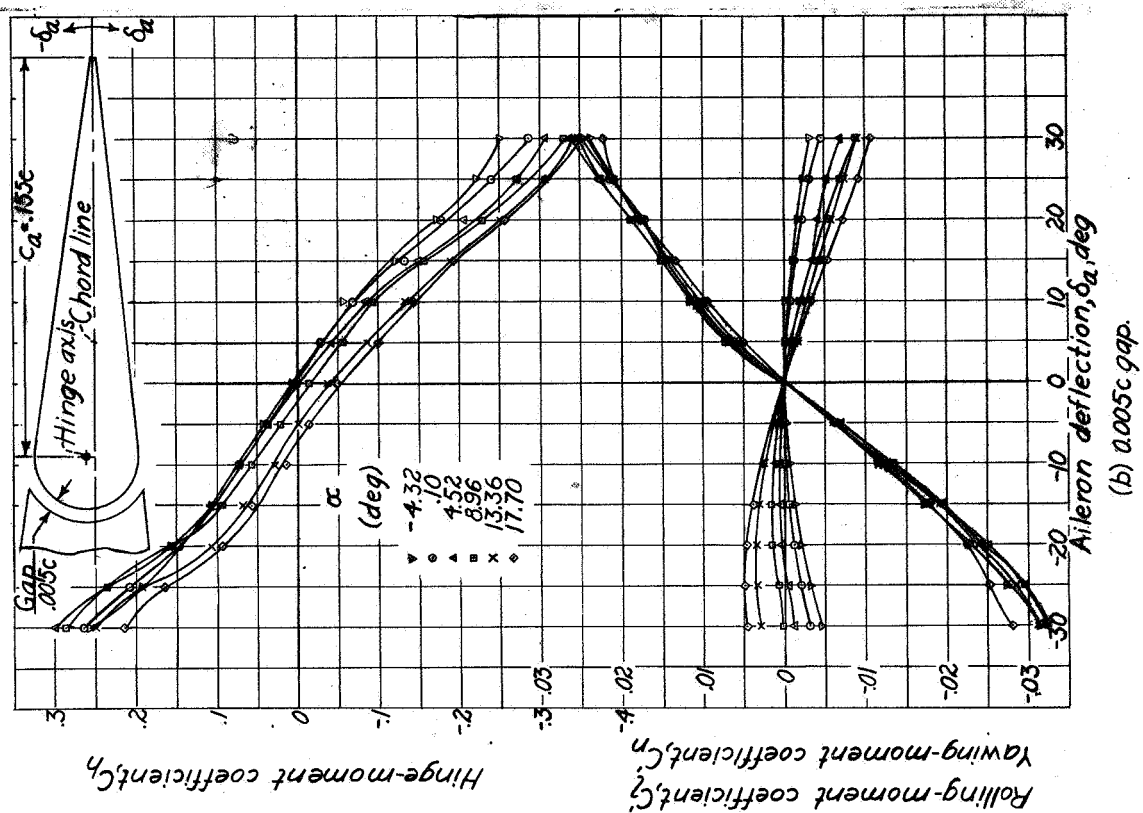
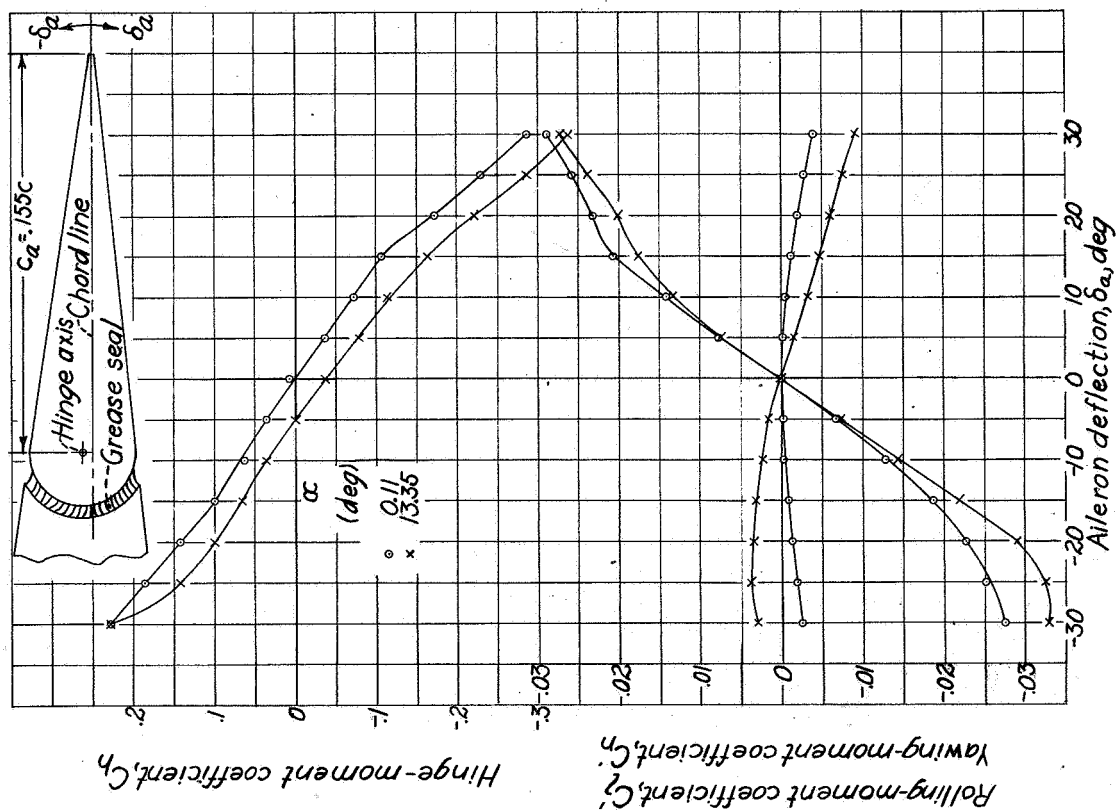


Fig. 7

Figure 7.- Concluded



(a) Sealed gap.

Figure 7.- Characteristics of the plain aileron on the tapered-wing model.

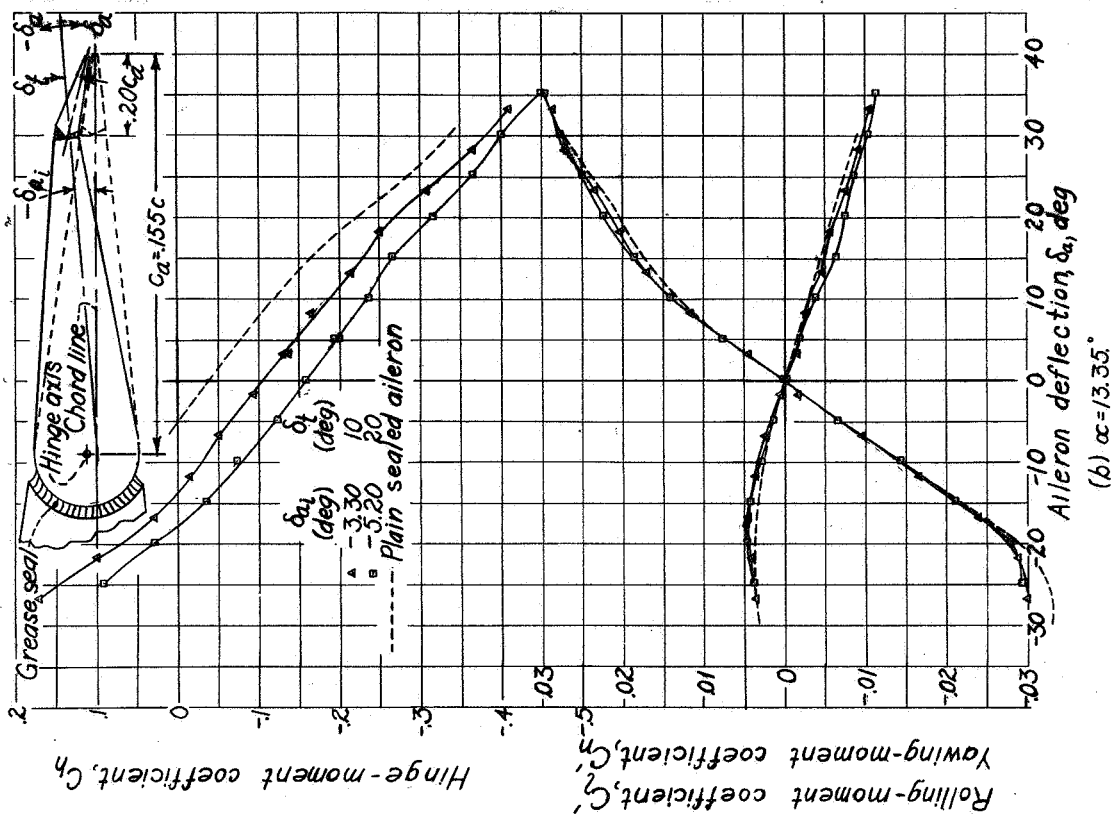


Figure 8.- Concluded.

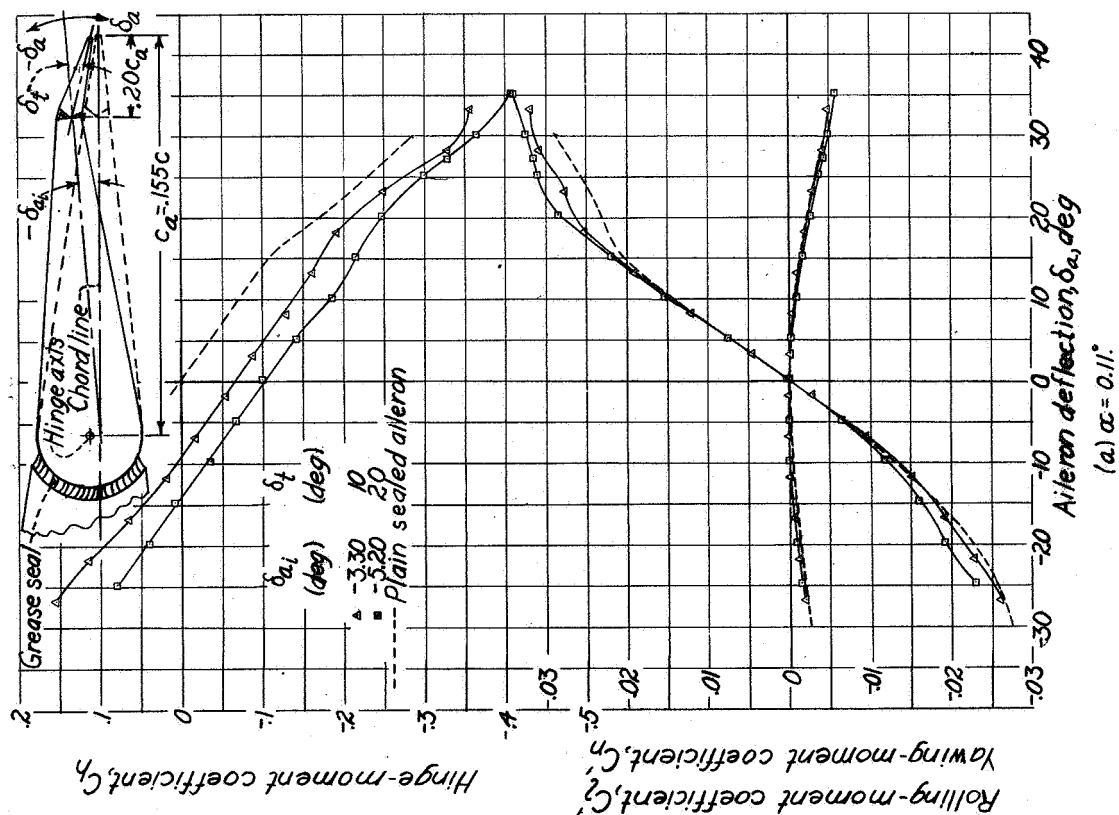
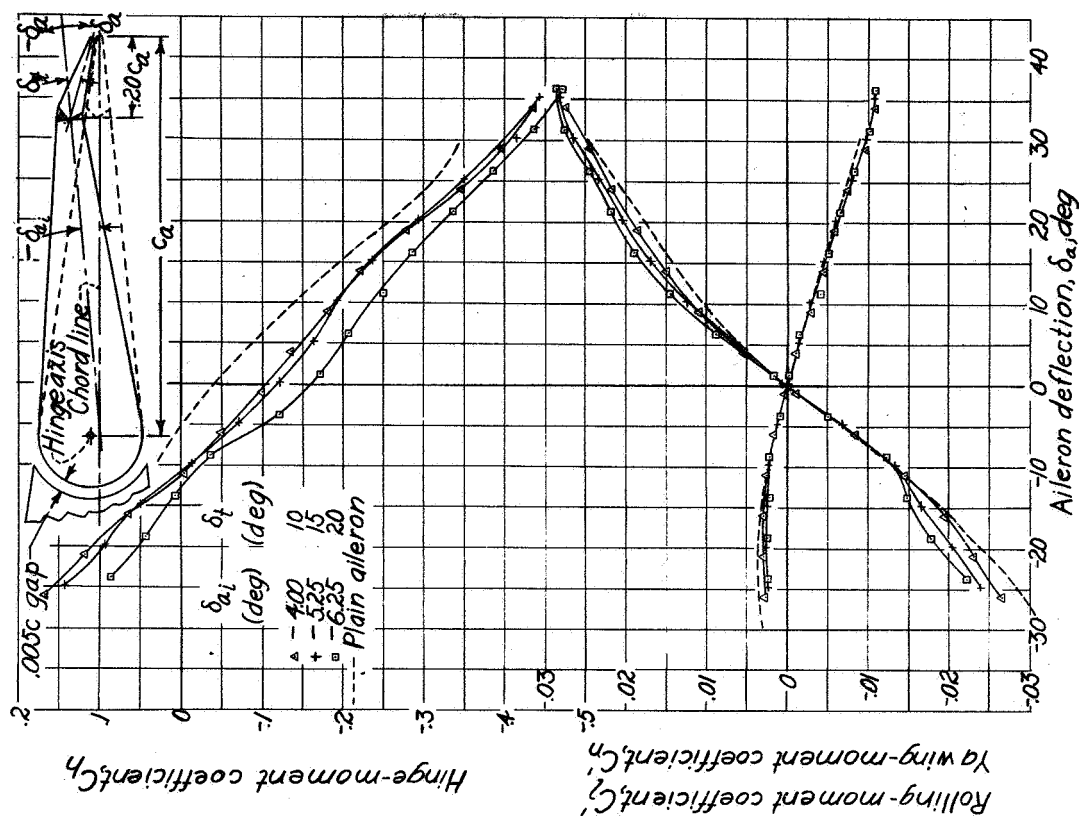
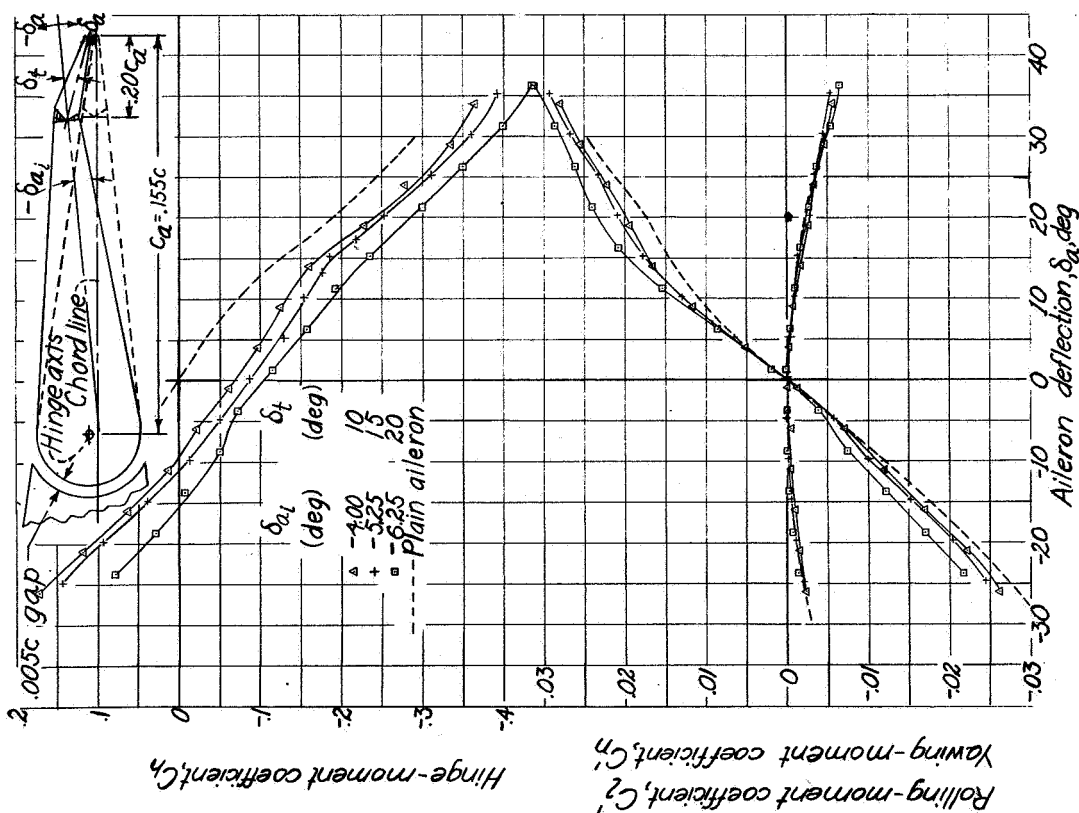


Figure 8.- Characteristics of the uprigged aileron with positive tab on the tapered-wing model. Sealed gap.



(a)  $\alpha = 0.10^\circ$

Figure 9.-Concluded.



(b)  $\alpha = 13.36^\circ$

Figure 9.-Characteristics of the uprigged aileron with positive tab on the tapered-wing model. 0.005c gap.

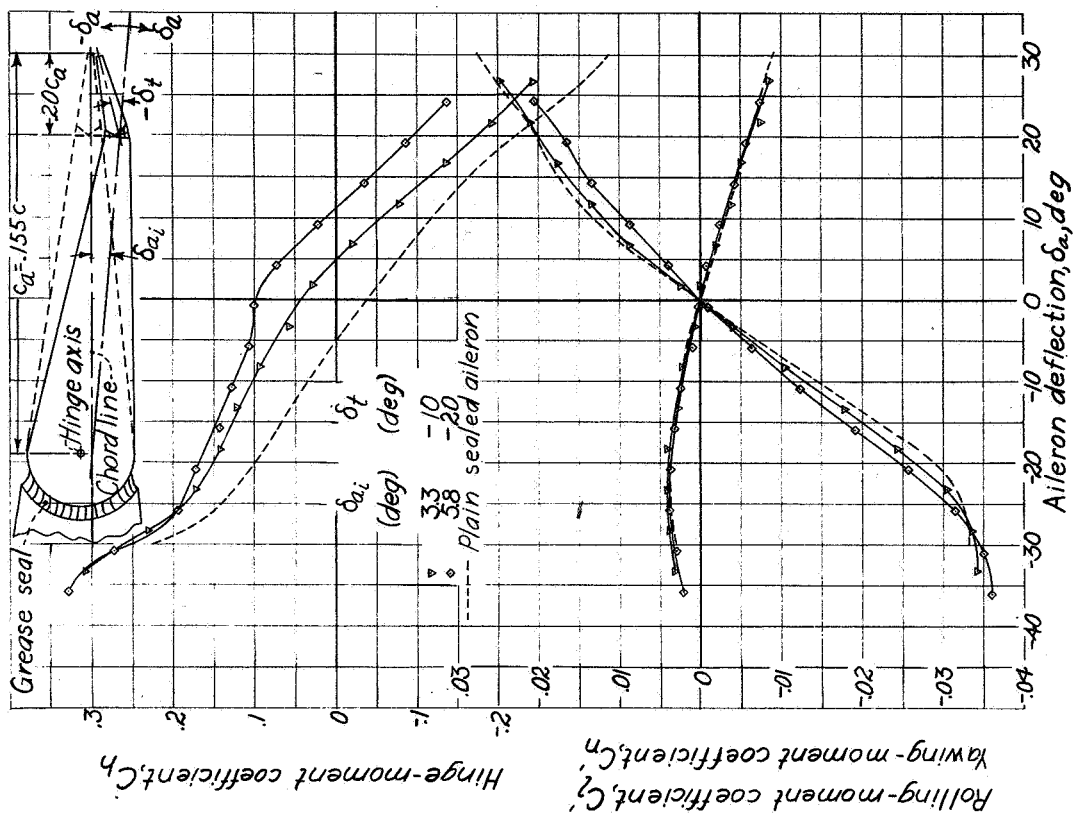
(a)  $\alpha = 0.11^\circ$ 

Figure 10.- Characteristics of the downrigged aileron with negative tab on the tapered-wing model. Sealed gap.

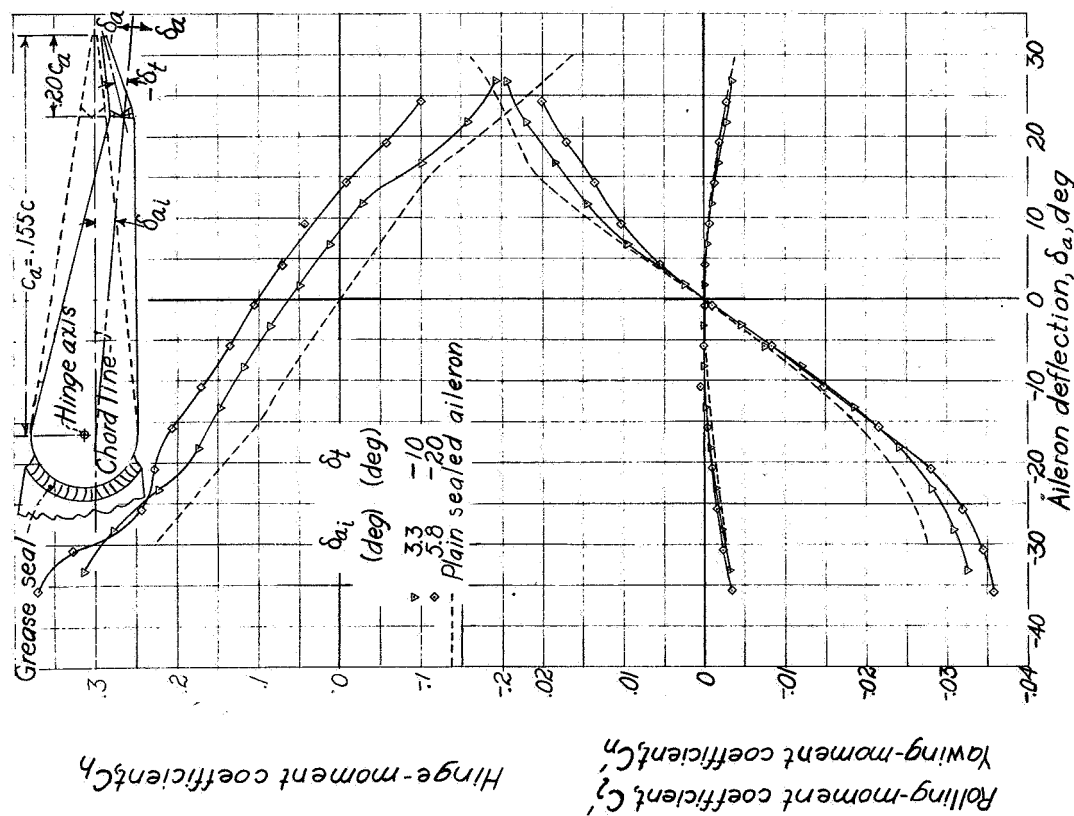
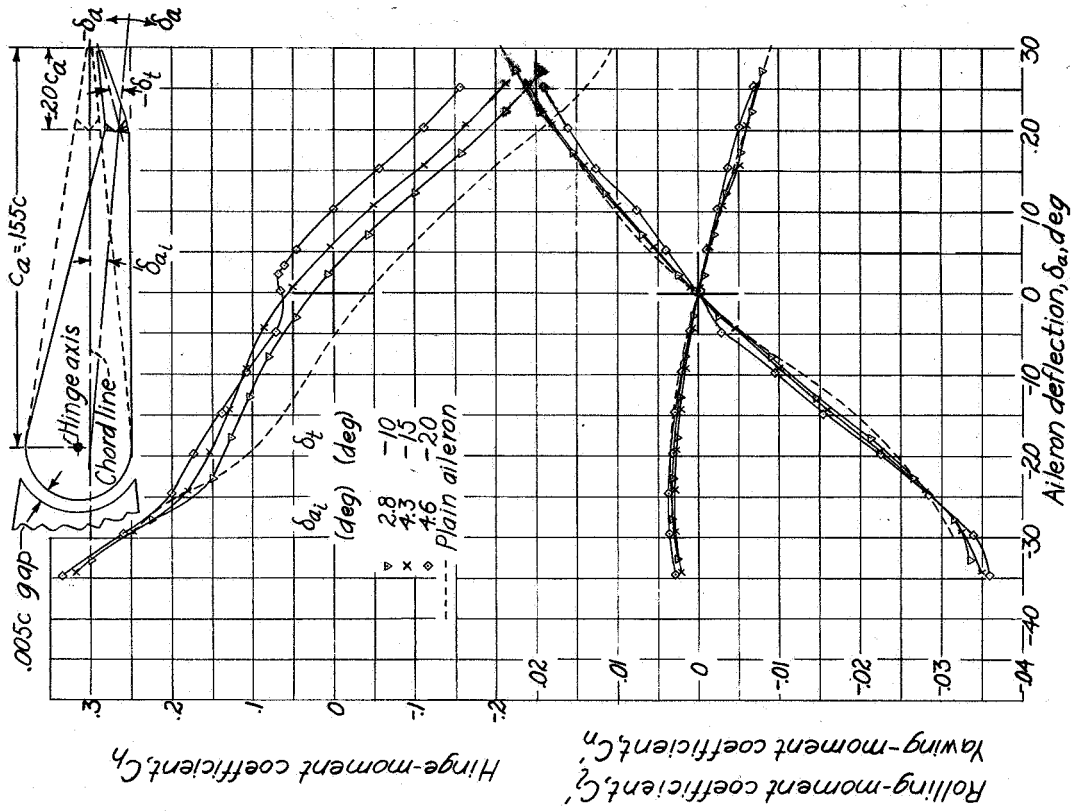
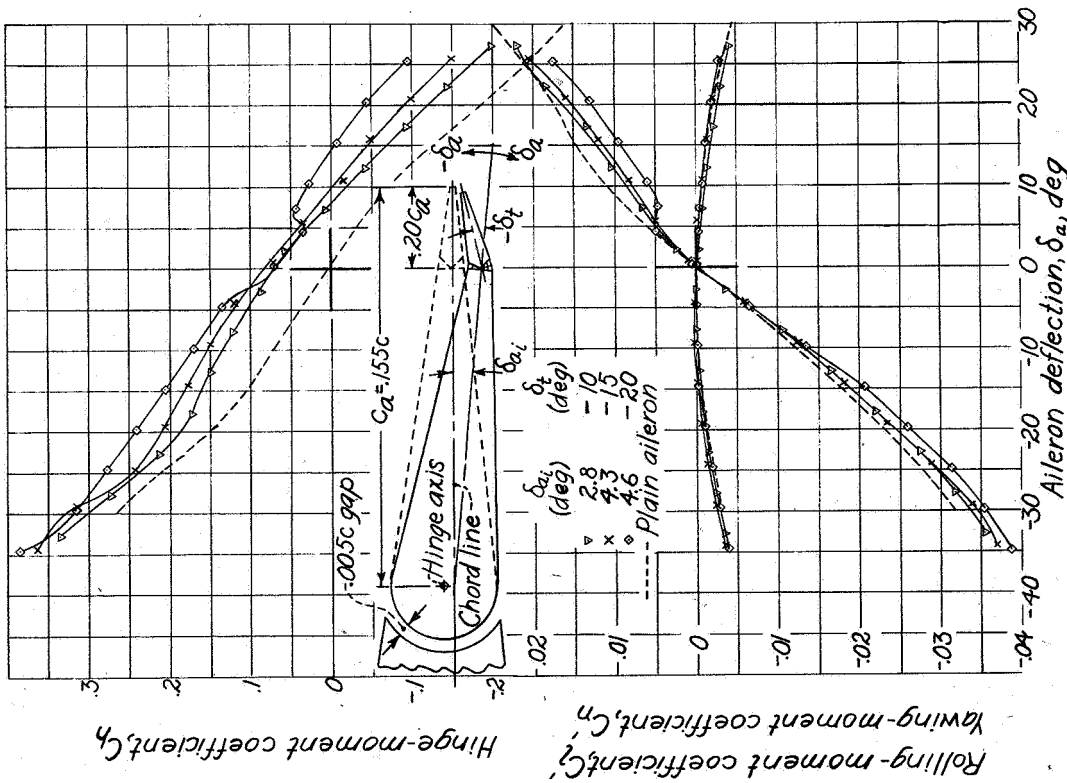
(b)  $\alpha = 13.35^\circ$ 

Figure 10.- Concluded.



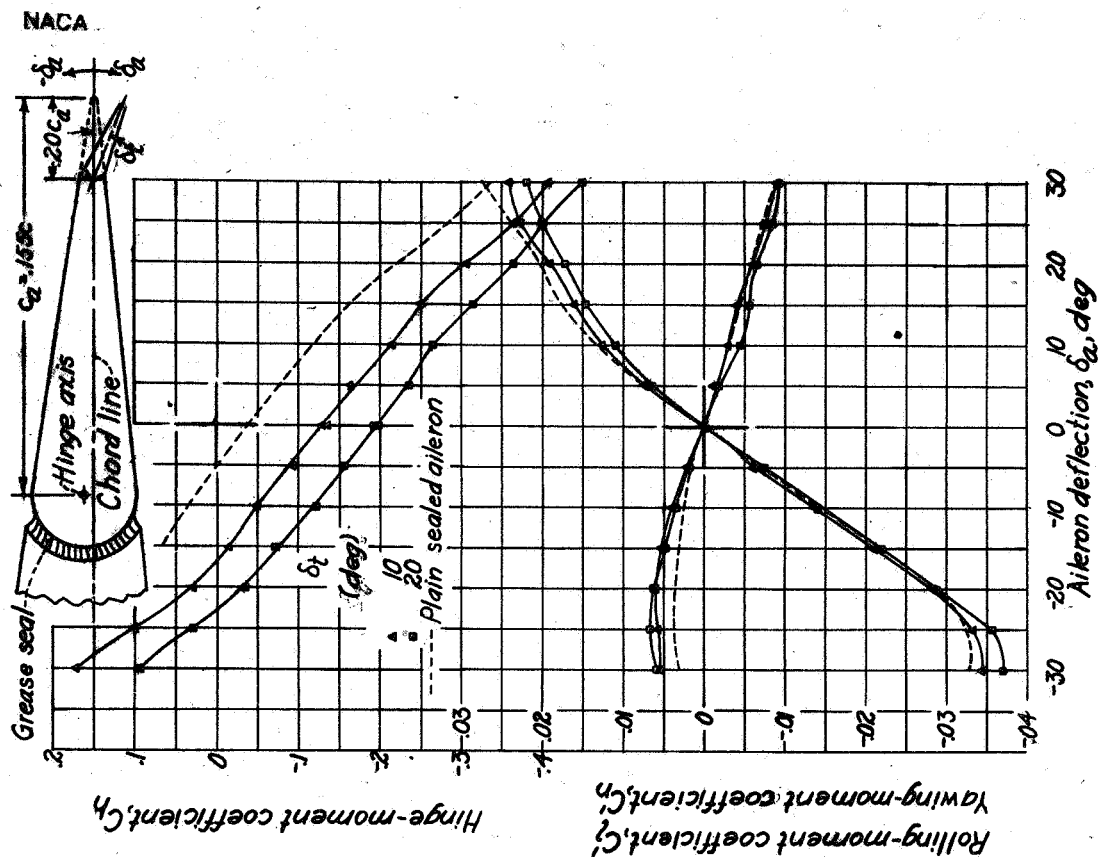
(b)  $\alpha = 13.36^\circ$

Figure 11.-Concluded.



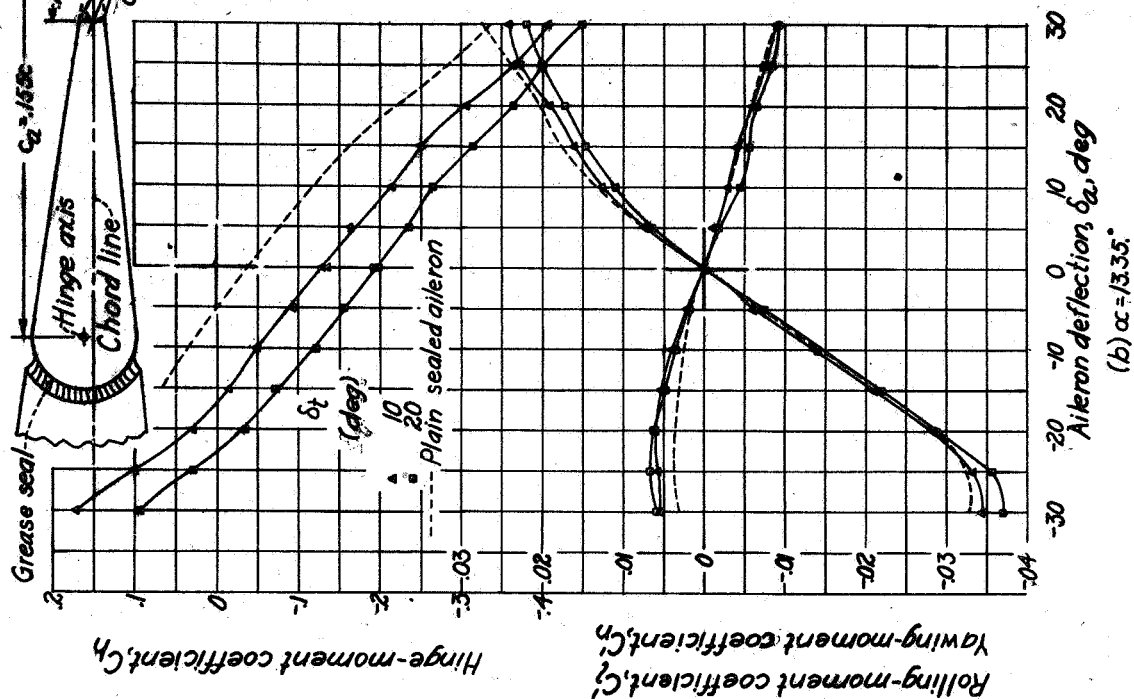
(a)  $\alpha = 0.10^\circ$

Figure 11.- Characteristics of the downrigged aileron with negative tab on the tapered-wing model. 0.005c gap.



(a)  $\alpha = 0.11^\circ$

Figure 12.- Characteristics of the neutrally rigged aileron with positive tab on the tapered-wing model. Sealed gap;  $\delta_a, 0^\circ$ .



(b)  $\alpha = 13.35^\circ$

Figure 12.- Concluded.

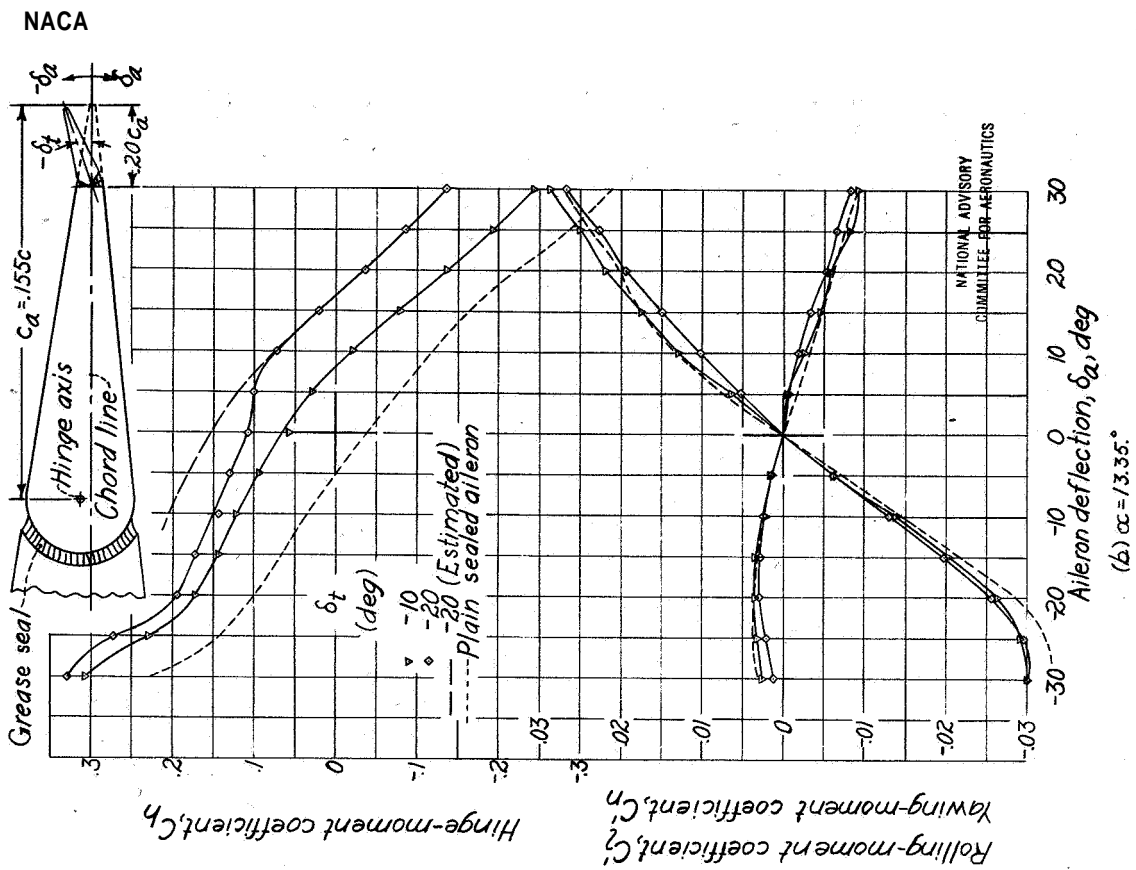


Fig 13

Figure 13.- Concluded.

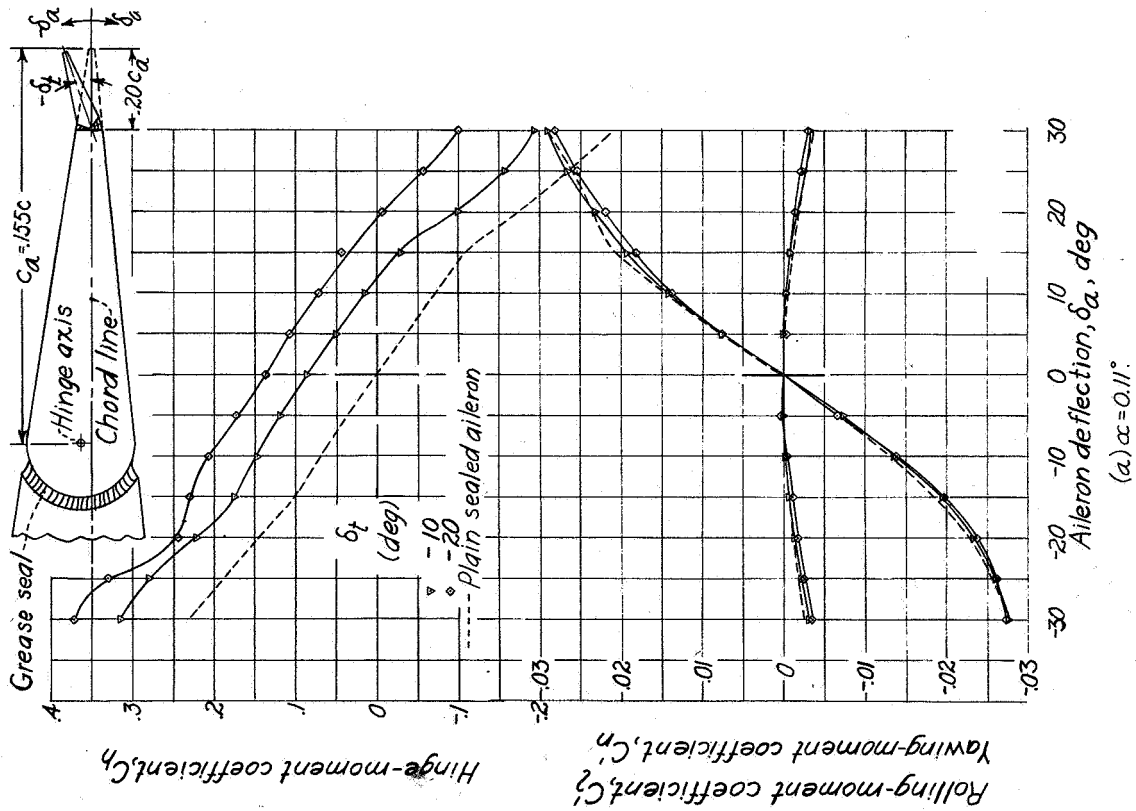
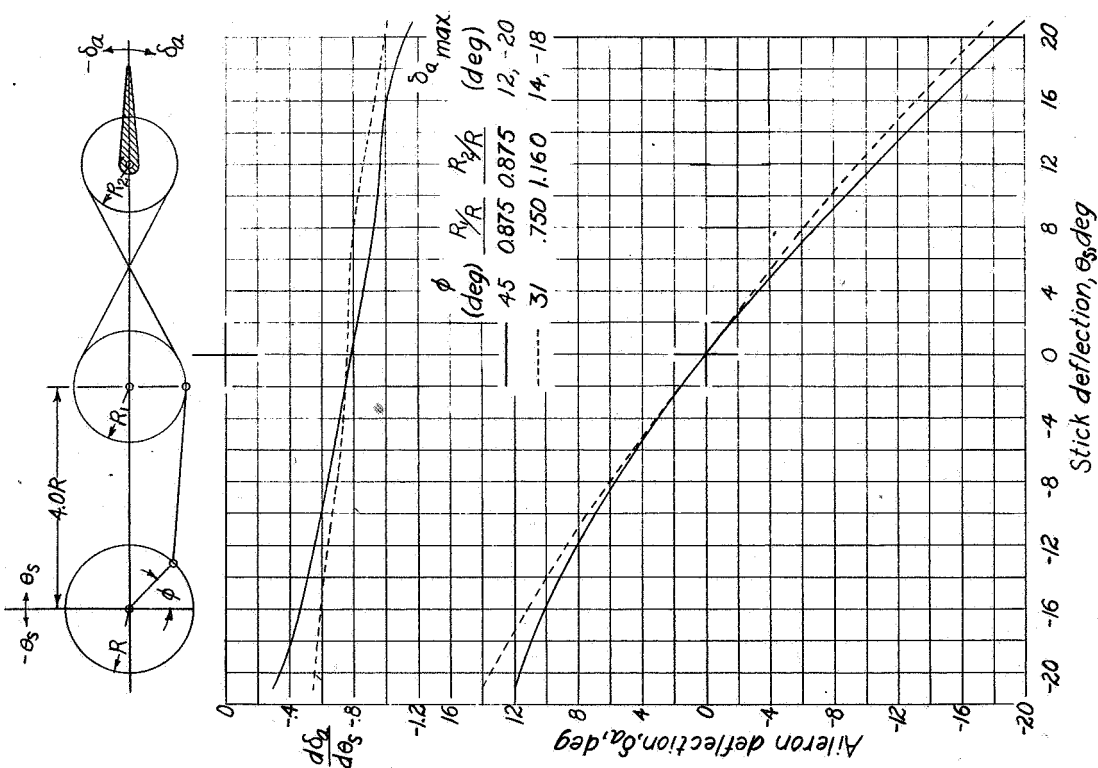
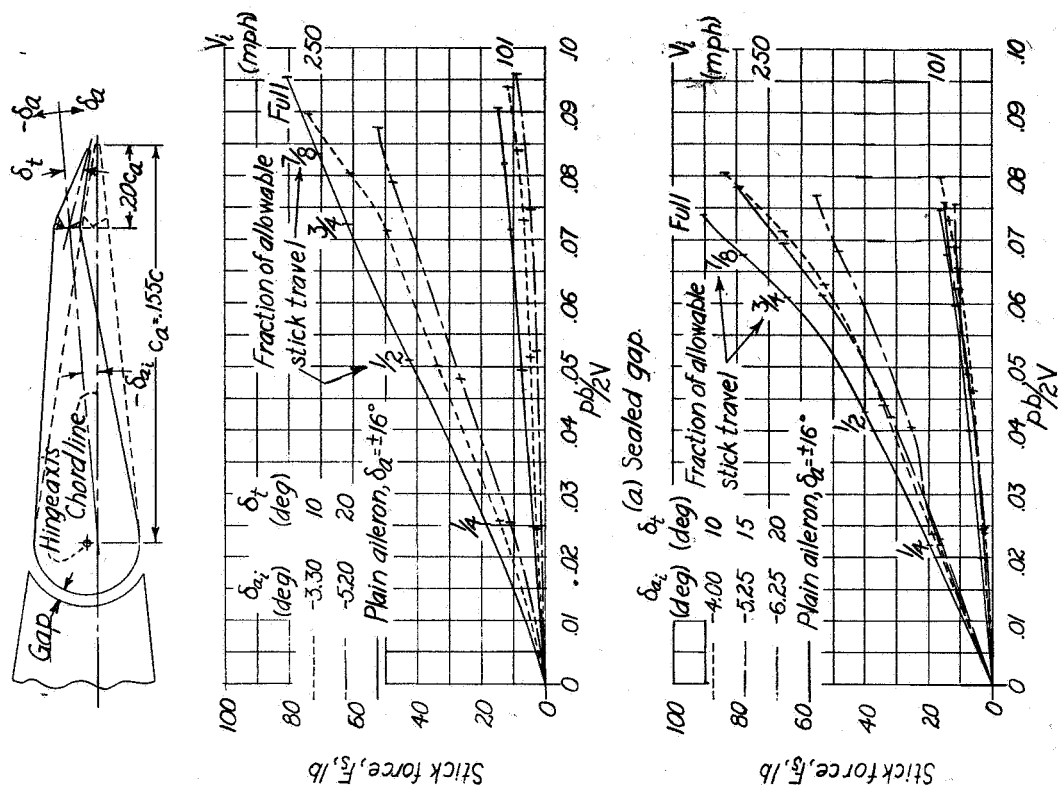


Figure 13.- Characteristics of the neutrally rigged aileron with negative tab on the tapered-wing model. Sealed gaps  $\delta_a$ ,  $0^\circ$





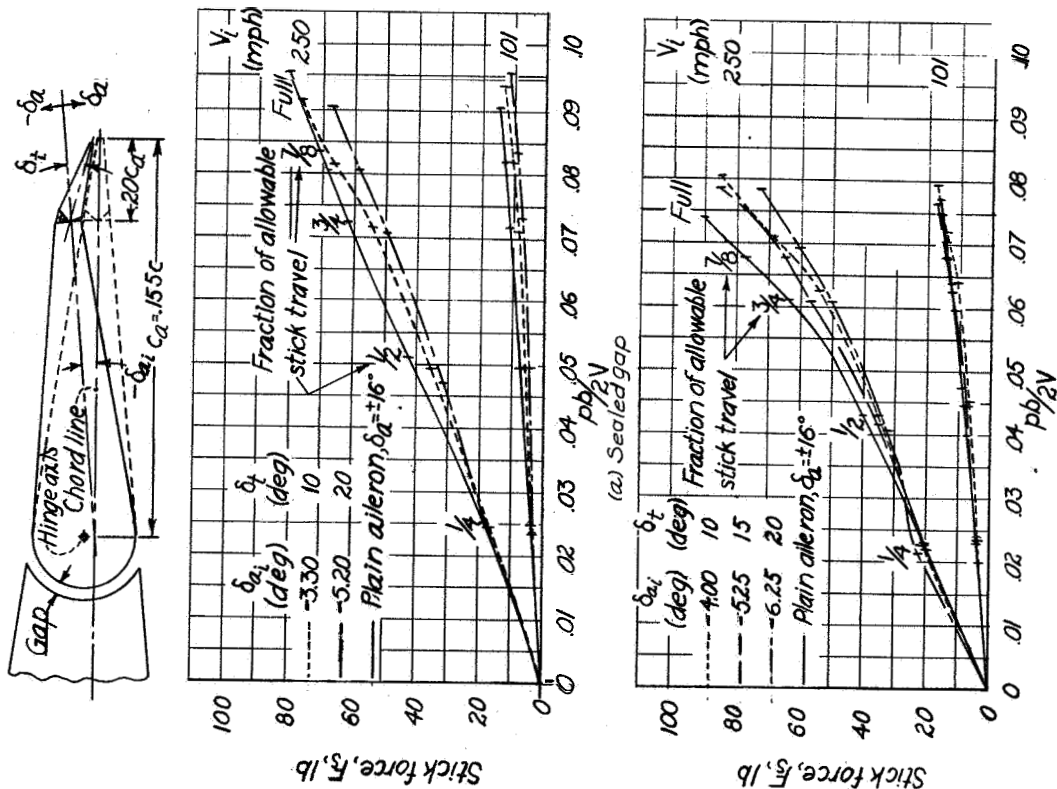


Figure 16.-Stick-force characteristics of the uprigged ailerons with positive tabs on the tapered wing. Conventional differential;  $\delta_a$  range,  $-18^\circ$  to  $14^\circ$ .

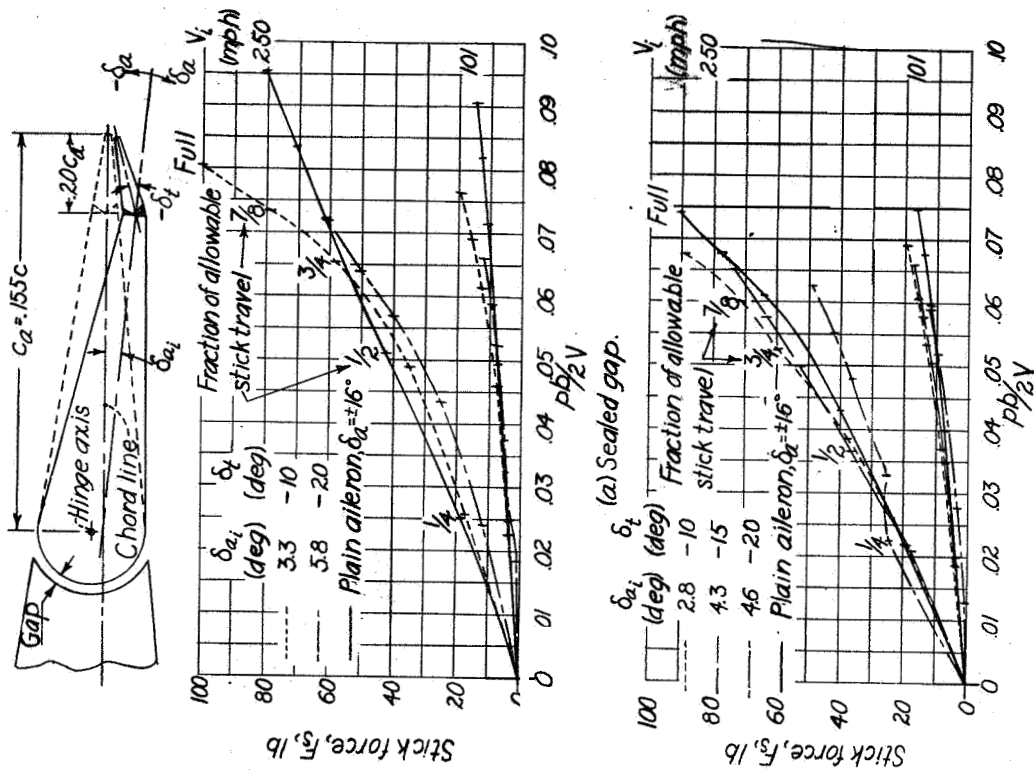


Figure 17.-Stick-force characteristics of the downrigged ailerons with negative tabs on the tapered wing. Reversed differential;  $\delta_a$  range,  $-12^\circ$  to  $20^\circ$ .

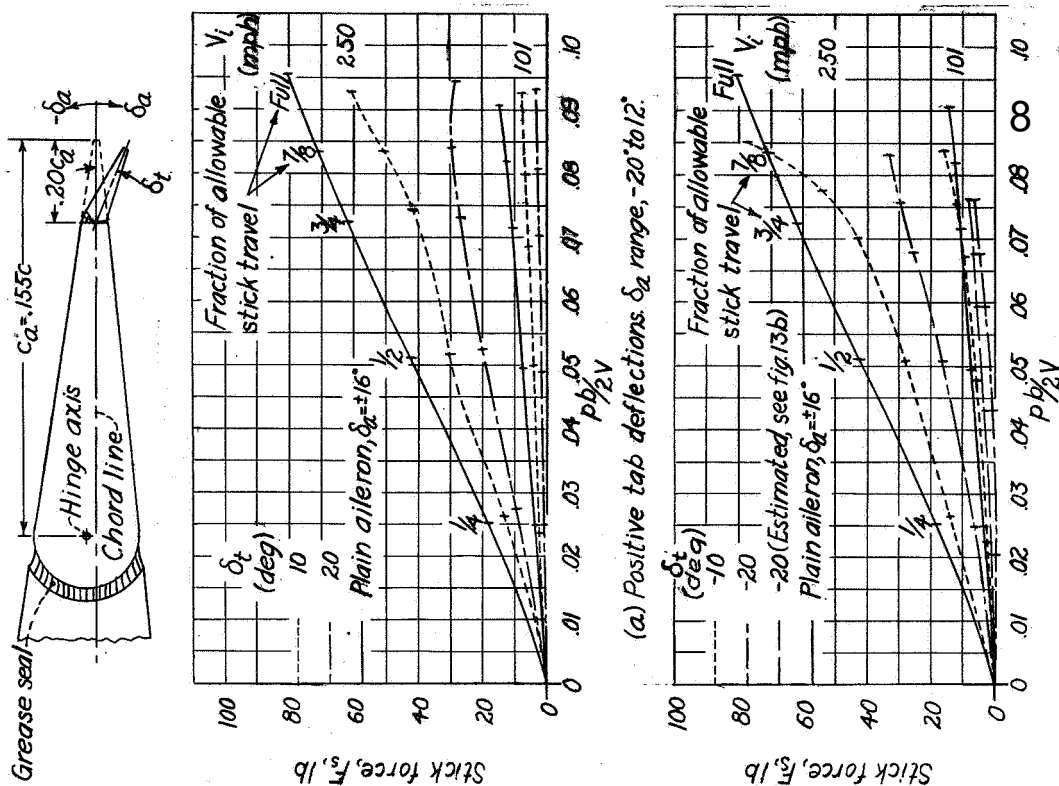


Figure 19.- Stick-force characteristics of the neutrally rigged ailerons with fixed tabs on the tapered wing. Sealed gap;  $\delta_{ai}$ ,  $0^\circ$ .

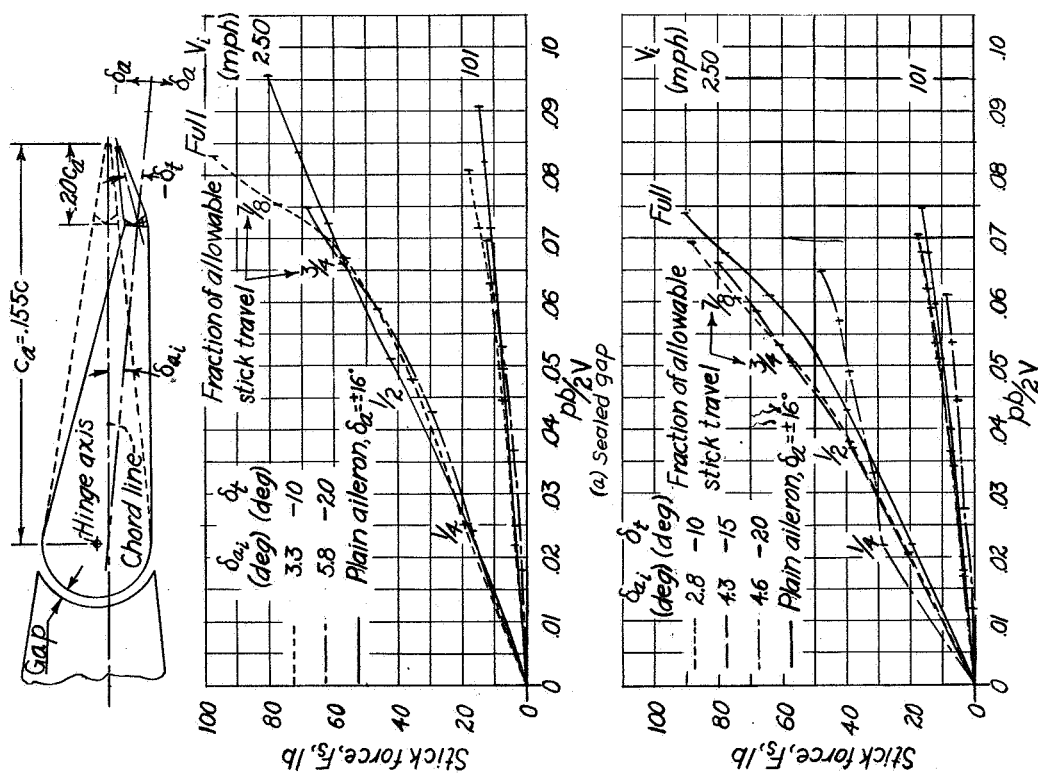


Figure 18.- Stick-force characteristics of the down rigged ailerons with negative tabs on the tapered wing. Reversed differential;  $\delta_{ai}$  range,  $-4^\circ$  to  $18^\circ$ .